Percolation properties of the Wolff clusters in planar triangular spin models

P. W. Leung* and Christopher L. Henley
Laboratory of Atomic and Solid State Physics, Cornell University, Ithaca, New York 14853
(Received 22 August 1990)

We formulate the Wolff algorithm as a site-bond percolation problem, apply it to the ferromagnetic and antiferromagnetic planar triangular spin models, and study the percolation critical behavior using finite-size scaling. In the former case the Wolff algorithm is successful as an accelerating algorithm, whereas in the latter case it is not. We found the percolation temperatures and the cluster exponents for both models. In the antiferromagnetic model, the percolation temperature is higher than the critical temperature of the spin system. The cluster exponents are found to be the same as the random two-dimensional (2D) percolation. In the ferromagnetic model, the percolation temperature agrees with the critical temperature, and the cluster exponents are different from the random 2D percolation, meaning that they are in different universal classes. For the ferromagnetic model we discuss the mechanism of the cluster growth in the regime of the Kosterlitz-Thouless transition. We also note a relation between the dynamic exponent and the percolation exponents.

I. INTRODUCTION

Ever since Swendsen and Wang[1] (SW) put forward their novel algorithm for the Potts model, various algorithms have been proposed[2–5] to reduce critical slowing down of spin systems using ideas from percolation theory. The original SW algorithm[1] is based on the Fortuin-Kasteleyn mapping[6] for site-bond percolation and the Potts model. Clusters of spins in the same states are grown and the whole clusters are flipped. Thus, a number of spins are updated in a single move and the correlation time is reduced. This was successfully applied to the ferromagnetic Potts model and the antiferromagnetic Ising model on a square lattice.[1] Later Wolff[4] introduced a single-cluster algorithm that, when applied to the Ising model, is similar to the SW algorithm except that only one of the SW clusters is flipped. This particular cluster is chosen with a probability proportional to its size. Wolff also introduced a generalization of the spin-flip operation in the Ising model to models with continuous degree of freedom and successfully applied it to the ferromagnetic XY and Heisenberg model.[4] Using a combination of the SW algorithm and the Wolff flips, Wang, Swendsen, and Kotecký[5] were able to deal with the antiferromagnetic three-state Potts model on a square and simple-cubic lattice. In all of the above cases, the systems are not frustrated and the new algorithms give a significantly smaller dynamical exponent than the Metropolis algorithm. A comparison of the efficiency between the SW and Wolff algorithm for the Ising model was done by Tamayo, Brower, and Klein[7] who found that, for $d > 2$, the Wolff algorithm is more efficient than the SW algorithm.

We have been motivated by an interest in techniques for acceleration of vector spin systems with competing interactions (frustration). An alternative method, Fourier acceleration, can speed up the relaxation of the long-wavelength modes of any continuous degree of freedom. It is successful in reducing critical slowing down in ferromagnetic and other unfrustrated spin systems.[8,9] However, frustrated systems commonly break discrete degrees of freedom in addition to the global continuous symmetry; in particular, the global symmetry group $O(n)$ for n-vector spin systems contains a reflection operation which is discrete. When Fourier acceleration was applied to such a system, it was found to be ineffective in accelerating the discrete degree of freedom.[10] The Wolff update is exactly a reflection, so there is an apparent possibility that it could be useful in updating these degrees of freedom. Unfortunately, our study has shown that the Wolff algorithm does not succeed in finding the right groupings of spins to be reflected.

While the previous works are concentrated on showing the efficiency of the new algorithms by finding the dynamical critical exponent, in this paper we present a study of the percolation properties of the clusters[11] in the Wolff algorithm. Instead of being used as an acceleration algorithm to reduce critical slowing down, we formulate the Wolff algorithm as a site-bond percolation problem. It is applied to the planar triangular spin model with ferromagnetic (FPT) and antiferromagnetic (AFPT) interactions, the latter being a frustrated system. We will show that, for the FPT model, T_p (the percolation temperature of the Wolff clusters) is equal to T_c (the critical temperature of the spin system), whereas $T_p > T_c$ for the AFPT model. Thus, in one case (FPT), the Wolff algorithm is successful in reducing critical slowing down while in the other case (AFPT) it is not. We will investigate the properties of the Wolff clusters in these two cases.

II. WOLFF ALGORITHM AS A PERCOLATION PROBLEM

Consider a classical planar spin system with Hamiltonian

$$H = -\beta J \sum_{\langle xy \rangle} \sigma_x \cdot \sigma_y \ . \tag{1}$$

Wolff[4] generalized the spin-flip operation in the Ising model to a continuous model by defining it to be a reflection about a direction orthogonal to a projection vector $\mathbf{r}$ in the spin space

$$\mathcal{R}(\mathbf{r})\boldsymbol{\sigma}_x = \boldsymbol{\sigma}_x - 2(\boldsymbol{\sigma}_x \cdot \mathbf{r})\mathbf{r} \ . \tag{2}$$

For a particular projection vector $\mathbf{r}$ which is chosen at random, we can identify the clusters in the system by visiting each nearest-neighboring bond $\langle xy \rangle$ and activating it with the probability

$$P(\boldsymbol{\sigma}_x, \boldsymbol{\sigma}_y) = 1 - \exp\{\min[0, -2\beta J(\mathbf{r}\cdot\boldsymbol{\sigma}_x)(\mathbf{r}\cdot\boldsymbol{\sigma}_y)]\} \ . \tag{3}$$

We then pick a spin at random. The cluster to which it belongs is called the Wolff cluster. The Wolff algorithm of sampling the spin configurations consists of continuously generating the Wolff clusters using random projection vectors and flipping them according to Eq. (2) as soon as they are generated. In this way we generate a series of spin configurations and a distribution of Wolff clusters n_s^*. It can be shown[4] that this satisfies the detailed balance and will sample spin configurations according to the partition function corresponding to the Hamiltonian in Eq. (1).

At high temperatures, the spins are less correlated and the cluster sizes are small. As the temperature is lowered, the spins become more ordered and the cluster sizes increase. We define the percolation temperature of the Wolff clusters T_p as the temperature at which spanning clusters start to appear in a large system. Therefore, we have two different critical temperatures in our system: the critical temperature of the spin system T_c and the percolation temperature of the clusters T_p. In our two-dimensional (2D) models, we consider T_c to be the Kosterlitz-Thouless[12] (KT) temperature for the FPT model. For the AFPT model, we consider T_c to be the temperature at which both discrete and continuous degrees of freedom[13] order. As in an ordinary percolation problem, we can define the following cluster properties for the Wolff clusters: the percolation probability P_∞ which is the fraction of spins belonging to the spanning cluster, the distribution of cluster size $n_s = N_s/N$, where N_s is the fraction of Wolff clusters with size s, and $N = L^d$ is the total number of spins in the lattice. Also, the cluster susceptibility χ_p is the second moment of the cluster distribution

$$\chi_p \equiv \sum_s s^2 n_s \ . \tag{4}$$

We will write the expectations $\langle \cdots \rangle$ with respect to the Wolff process. A given Wolff cluster has one chance to be grown for each site that can be hit; thus, the probability of hitting a Wolff cluster of size s is

$$n_s^* = \frac{s}{N} N_s = s n_s \ , \tag{5}$$

i.e., the clusters are hit with probability proportional to their sizes. Then we can write

$$\chi_p = \sum_s s n_s^* = \langle s \rangle \ . \tag{6}$$

Here the temperature of the system plays the role of the percolation probability p in the ordinary percolation problem. The system is above the percolation threshold when T is below T_p and vice versa.

To make the computational problem well defined, we need a working definition of P_∞ when $L < \infty$. If we found all clusters simultaneously as in SW,[1] then we could use the standard approach of taking the largest cluster as the "infinite" spanning cluster. However, with the algorithm of Ref. 4, we only generate one cluster at a time; therefore, we have chosen to extract P_∞ from the function n_s^*. We suppose there is a cutoff cluster size s_c, above which the Wolff clusters are considered to be spanning clusters. Now, in the limit $L \to \infty$, we note that P_∞ is related to n_s^* in two independent ways; we generalize these ways to finite L, and then we fix s_c by requiring that both ways give the same value of P_∞. The two ways are the following: (i) The size of the spanning cluster is $P_\infty N$; thus, we require

$$P_\infty = \frac{1}{N}\langle s \rangle_{s>s_c} = \frac{1}{N}\frac{\sum_{s_c}^{N} s n_s^*}{\sum_{s_c}^{N} n_s^*} \ . \tag{7}$$

(ii) On the other hand, since P_∞ is the fraction of all spins which belong to the spanning cluster, the probability that a Wolff hit is on the spanning cluster is P_∞. Thus, we require

$$P_\infty = \mathrm{Prob}(s > s_c) = \sum_{s_c}^{N} n_s^* \ . \tag{8}$$

[Note the normalization $\sum_1^N n_s^* = 1$ follows from (5).]

Note that P_∞ from Eq. (7) increases as s_c increases, whereas P_∞ from Eq. (8) decreases as s_c increases, so there is a unique solution of s_c for which (7) and (8) are equal. This uniquely defines an estimator $\hat{P}_\infty$ from the distribution of Wolff clusters n_s^*.

As in ordinary percolation problems, we make the following scaling assumptions:

$$P_\infty = L^{-\beta_p/\nu_p} f(tL^{1/\nu_p}) \ , \tag{9}$$

$$\chi_p = L^{\gamma_p/\nu_p} g(tL^{1/\nu_p}) \ , \tag{10}$$

$$n_s^* = s^{-\tau_p^*} h(ts^{\sigma_p}, tL^{1/\nu_p}) \ , \tag{11}$$

where $t = |1 - T/T_p|$ and

$$\tau_p^* = \tau_p - 1 \ . \tag{12}$$

Equation (12) results from Eq. (5) and so the Wolff exponent τ_p^* is smaller than the cluster exponent τ_p by 1. Observe that in the limit $t \to 0$, Eq. (11) implies

$$n_s^* = s^{-\tau_p^*} \tilde{h}(ts^{\sigma_p}) \ . \tag{13}$$

This is consistent with the fractal scaling

$$s \sim R^D \tag{14}$$

for clusters of diameter R only if the fractal dimension D

obeys the relation $D\nu\sigma=1$. It can be shown by inserting (11) into (7) and (8) that our estimator $\hat{P}_\infty$ indeed satisfies (9).

III. RESULTS

We now consider an AFPT model with Hamiltonian (1) and $J=-1$. The T_c for this system was previously determined to be 0.505 ± 0.005.[13] We generate the Wolff clusters according to the algorithm in Ref. 4, which is an equivalent, but more efficient, version of the algorithm described above. A "Wolff step" consists of generating a Wolff cluster and flipping it to obtain a new spin configuration; the number of spins updated in one Wolff step is equal to the size of the Wolff cluster. The following runs are for 100 000 Wolff steps. The system sizes are $L=12$, 18, 24, 36, 48, and 72, where $N=L^2$. The spin configurations are in a parallelogram cell with periodic boundary conditions. Figure 1 shows a typical distribution of the cluster sizes at a temperature above T_p, (i.e., below percolation threshold). For intermediate cluster sizes, n_s^* follows a power law. Figure 2 shows the scaling plots for P_∞, χ_p, and n_s^*. It is clear that the distribution of the Wolff clusters depends on the size L. Hence, there are two arguments in the scaling function h in Eq. (11). But, for $s \ll L^d$, one will expect that the dependence of n_s^* on L is not important. In Fig. 2(c), only the data points for $L=72$ (which is our largest system) are plotted. T_p and the critical exponents are found by adjusting their values to achieve optimal collapsing of the data points into a single curve. Their uncertainties are estimated by varying their values and visually determining the maximum deviation so that the data collapsing is still acceptable. From the scaling plots we find that $T_p=1.037\pm0.002$. The cluster exponents are tabulated in Table I. Note that values of ν_p are independently determined from Figs. 2(a) and 2(b), and they turn out to be the same. Also listed in Table I are the critical exponents for the 2D random percolation calculated from

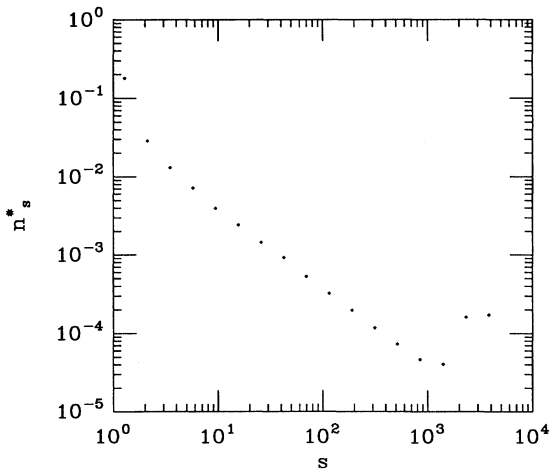

FIG. 1. Distribution of Wolff clusters n_s^* for the AFPT model with $L=72$ at $T=1.04$.

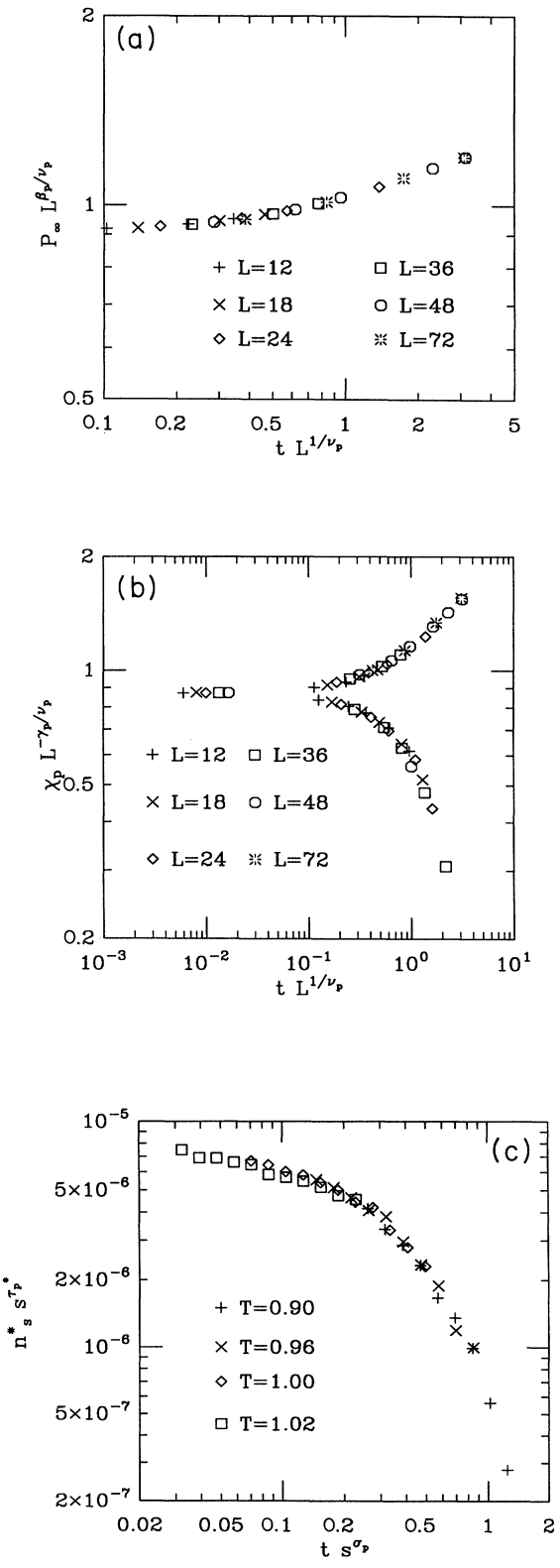

FIG. 2. Finite-size scaling plots for the AFPT model: (a) P_∞, (b) χ_p; the upper and lower branches are for $T<T_p$ and $T>T_p$, respectively. (c) Scaling plot (for $L=72$ only) of cluster size distribution n_s^*.

TABLE I. Critical exponents for the Wolff clusters as found from the scaling plots in Figs. 2 and 3 for the AFPT and FPT models, respectively. D is the fractal dimension. The values for 2D percolation are from Ref. 17. τ_p is obtained from τ_p^* through Eq. (12), D is calculated from Eq. (17). The other exponents are obtained from the scaling plots.

Exponent	AFPT	FPT	2D percolation
β_p	0.140±0.004	0.25±0.03	$\frac{5}{36}=0.139$
ν_p	1.355±0.005	2.5±0.2	$\frac{4}{3}=1.333$
γ_p	2.41±0.02	4.5±0.4	$\frac{43}{18}=2.389$
τ_p	2.01±0.02		$\frac{187}{91}=2.055$
σ_p	0.39±0.02		$\frac{36}{91}=0.396$
D	1.88±0.02	1.90±0.01	$\frac{91}{48}=1.896$

the conjectures of den Nijs,[14] Pearson,[15] and Nienhuis *et al.*[16] These values are believed to be exact.[17] We observe that they agree quite well. Thus, the exponents numerically obey the usual scaling laws

$$\beta_p=(\tau_p-2)/\sigma_p\ ,$$
$$-\gamma_p=(\tau_p-3)/\sigma_p\ , \tag{15}$$

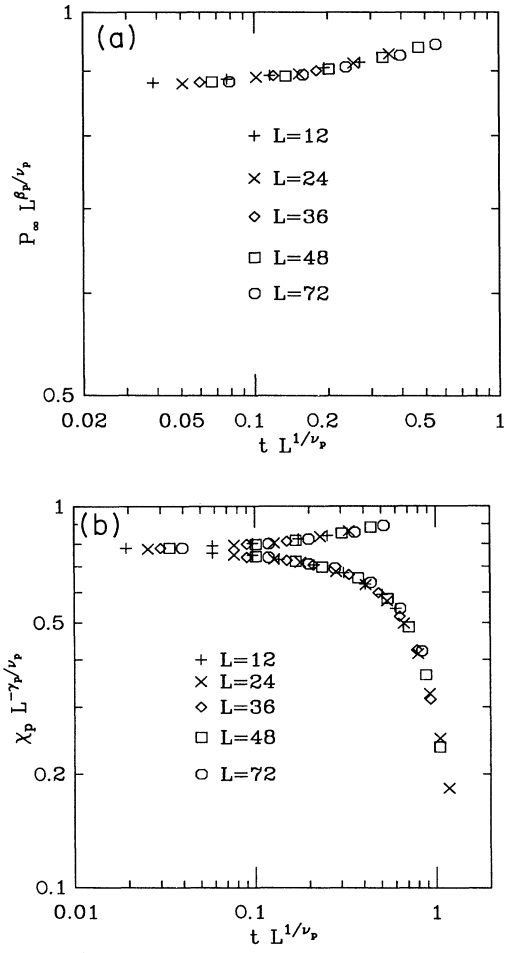

FIG. 3. Finite-size scaling plots for the FPT model, (a) P_∞ and (b) χ_p.

and the hyperscaling law

$$d\nu_p=\gamma_p+2\beta_p\ . \tag{16}$$

The fractal dimension D is obtained through the relation

$$D=(\gamma_p+\beta_p)/\nu_p\ . \tag{17}$$

We conclude that the Wolff clusters in an AFPT model are in the same universality class as random 2D percolation.

We next consider the FPT model with Hamiltonian (1) and $J=+1$. T_c was previously determined to be 1.39 ± 0.02.[18] Figure 3 shows the scaling plots for P_∞ and χ_p. (Attempts to make n_s^* data collapse on a scaling plot were unsuccessful.) From these plots we determined T_p to be 1.40 ± 0.02. Note that the uncertainty in T_p in this case is much larger than that in the AFPT model. This is because ν_p is larger in the present case and consequently the coefficient L^{1/ν_p} in the argument of the scaling functions (9) and (10) has a smaller range of accessible values, leading to a larger uncertainty in t.

The cluster exponents from the FPT model are also summarized in Table I. Hyperscaling (16) is again found to be satisfied numerically. Since we could only fit three independent exponents β_p, ν_p, and γ_p in this case, we cannot check the scaling laws (15). We observe that T_p agrees with T_c and the different exponent values show this system is in a different universality class from random 2D percolation. It is intriguing that β_p, ν_p, and γ_p are all larger than those of uncorrelated percolation by about the same factor ~ 1.85.

IV. DISCUSSION

A. AFPT model

In the AFPT model, we notice that $T_p > T_c$. The Wolff clusters percolate when the temperature is still appreciably higher than T_c. At temperatures near T_c, the cluster distribution is dominated by either very small clusters or infinite clusters. Thus, a great deal of computer time is spent in growing the infinite clusters, which, when flipped, have the net effect of updating those spins in the holes of the clusters only. This makes the algorithm very inefficient around T_c. At T_p, which is high compared with T_c, the spin correlation length is short and one may expect that the site-bond percolation resembles the random percolation. Hence, we expect the percolation of the Wolff clusters to be in the same universal class as the random 2D percolation, as confirmed in the exponents of the Wolff clusters.

B. FPT model

It is known from an exact mapping that, for the unfrustrated Ising and Potts model (where the acceleration algorithms has been successfully applied), $T_p=T_c$.[6,19] In the case of the ferromagnetic XY model, previous work[4] showed numerically that the Wolff algorithm successfully accelerated the dynamics near T_c, and by the argument at the beginning of Sec. V (below), this indicates that

$T_p = T_c$. Our result directly confirms that $T_p = T_c$ for the FPT model. At T_c the spin-correlation length diverges and the site-bond percolation changes to another universality class, as shown in the exponents of the Wolff clusters.

In general dimension d, we can distinguish two scenarios for what limits the size of Wolff percolation clusters in the FPT model. *Scenario 1:* large clusters become exponentially unlikely as they involve the product of many probabilities which are small compared to unity. This case is familiar, since it occurs in ordinary uncorrelated percolation. *Scenario 2:* a FPT system can be broken into "domains" by "domain boundaries" with respect to some projection vector **r**. These are boundaries separating regions where the spin components along **r** are of opposite signs. Within a given domain, the projection of every spin onto the Wolff projection vector **r** has the same sign and the Wolff clusters cannot jump across the domain boundaries.[20] Then, in this scenario, the clusters are limited by the domain boundaries, i.e., a typical Wolff cluster percolates and has a nonzero density through most of the interior of a domain.

Let us consider scenario 1. Since the cluster growth is not stopped by the domain boundaries but by the accumulation of the probabilities of broken bonds in the interior of the domains, we expect $\xi_p < \xi$. If $T_p \leq T_c$, we do not expect to find the same exponents as in ordinary percolation because the bond probabilities depend on the spin fluctuations, and near T_c these develop long-range correlations. It has been shown[21] that, for random bond percolation where the occupations p_x have long-range two-point correlations

$$\langle p_x p_y \rangle - p^2 \sim |x-y|^{-a} , \tag{18}$$

the correlations are relevant (changing all the exponents) if $a < 1/\nu_p$. In this case, the new correlation length exponent is $\nu' = 1/a > \nu_p$. The fact that we do not have an increased value of ν_p for the FPT case as compared to random percolation is consistent with this point of view, which would conclude that $a = 1/\nu_p \approx 0.8$. On the other hand, the KT theory[12] implies a decay of spin correlations (due only to spin waves)

$$\langle \sigma_x \sigma_y \rangle \sim |x-y|^{-\eta_{\mathrm{KT}}} , \tag{19}$$

with $\eta_{\mathrm{KT}}(T) = \frac{1}{4}$ at $T = T_c$. In view of the nonlinear relation (3) and the possible importance of higher than two-point correlations, it is not clear to us how (18) might be related to (19).

Note that, in scenario 1, it would be somewhat surprising to find $T_c = T_p$ exactly. Even in the long-range correlated percolation models, the critical fraction p_c is still between 0 and 1. Thus, one would not expect the onset of long-range correlations in the percolation to make a sudden qualitative change so that the system reaches percolation. Therefore, the observation that $T_p = T_c$ argues strongly for scenario 2.

Let us now consider scenario 2. For $d = 2$, it has been noted by Brower *et al.*[20] that every vortex must sit on a domain boundary; it is also clear that vortices of + and − signs must alternate along the domain boundary, and domain boundaries do not intersect. Then a single bound vortex pair typically produces a domain boundary loop so the domain diameter is comparable to the vortex spacing. Near T_c where there are vortices on many length scales, we must be more careful about this picture. The low-order equations of the KT renormalization group implicitly assume a separation of length scales between vortices; given a cutoff b, it is assumed that all vortices with spacing closer than b can be uniquely grouped into $(+,-)$ pairs and that they affect larger scales only by a renormalization of the effective spin stiffness constant. The corresponding domain picture is then hierarchically nested: every bound pair of two vortices must be connected by a domain boundary; smaller bound pairs can occur between the two vortices, but no larger bound pairs can occur between them. A schematic picture is shown in Fig. 4. It turns out that the KT correlation length is, in fact, the separation of the largest vortex pairs, i.e., the typical separation of unbound vortices.[12] At larger scales the vortices are unbound and random. At this point the domain boundaries connect nearby vortices randomly and we expect the domain size to be comparable to the spacing of unbound vortices. But the percolation correlation length is the cutoff of the cluster distribution. Thus, within scenario 2 where clusters are identified with domains, we get $\xi_p \sim \xi$.

In the case of ordinary uncorrelated percolation (at criticality), if we rescale the system, the cluster distribution is constant. In other words, clusters have a self-similar distribution; the density of clusters of size greater than R^D scales as R^{-d}, which implies

$$n(s) \sim s^{-(d/D+1)} , \tag{20}$$

which, in turn, implies the hyperscaling relation. However, for vortex pairs in the KT theory, the vortex pair den-

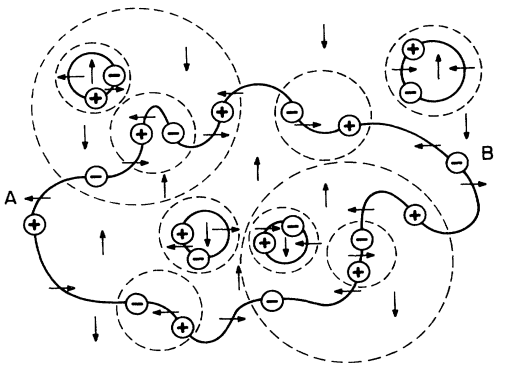

FIG. 4. Schematic picture of domain walls (solid lines) in a hierarchical configuration of bound vortices. Vortices are marked "+" and "−" according to their sign; a dashed circle encloses each bound pair. The Wolff projection vector **r** is taken to be vertical. The up and down arrows label domains in which the spins have positive and negative projections on **r**; along the domain walls the spin directions are strictly horizontal, in the sense marked by the horizontal arrows. Under further coarse graining, this configuration would be mapped to a single loop of domain wall connecting vortices A and B.

sity is proportional to y^2, where $y=e^{-E_c/T}$ is the vortex fugacity and E_c is the vortex core energy; the distribution can look the same on all length scales only if $y\rightarrow$const. Now, the KT recursion relations[12] have the form

$$\frac{dy}{dl}\sim(T-T_*)y\ ,\qquad \frac{dT}{dl}\sim y^2\ , \tag{21}$$

near the fixed point at T_*, where $b\sim e^l$ is the cutoff length scale. They iterate to a fixed point where $y=0$. So, under scenario 2, it follows that the cluster distribution is not exactly self-similar but must be corrected by a prefactor y^2. To be more precise, at T_c, the point where Eq. (21) iterates to $T=T_*$, they turn out to have a singular solution $y(l)\sim 1/l$. Thus, at T_c the distribution of vortex pairs is self-similar except for a logarithmic prefactor $\sim 1/(\ln R)^2$. Under scenario 2, and assuming that the fractal dimension relation (14) is still valid, we note $\ln R\sim\ln s$ and so conclude that the cluster size distribution ought to have the form

$$n(s)\sim s^{-(d/D+1)}/(\ln s)^2\ . \tag{22}$$

Since (22) is just modified by a logarithmic correction, there is no important effect on other scaling assumptions and on exponent relations which did not involve ν_p.

Under scenario 2, we must change the way t enters in the scaling assumptions. The scaling assumptions (9) and (10) become

$$P_\infty=L^{-x}f'(e^{-c/t^{1/2}}L)\ , \tag{23}$$

$$\chi_p=L^y g'(e^{-c/t^{1/2}}L)\ , \tag{24}$$

where c is nonuniversal. The scaling plots of these forms are shown in Fig. 5. There is apparently no visible difference on the quality of the fits in Figs. 3 and 5. The exponents are found to be

$$x=0.100\pm0.005\ ,\qquad y=1.78\pm0.01\ ,\qquad c=2.2\pm0.2\ . \tag{25}$$

The values of β_p/ν_p, γ_p/ν_p, and ν_p as determined from Fig. 3 are 0.100 ± 0.005, 1.80 ± 0.01, and 2.5 ± 0.2, respectively. Note that x, y, and c are close in value to β_p/ν_p, γ_p/ν_p, and ν_p fit from the power-law form in Sec. III. In the KT theory,

$$\chi\sim\xi^{2-\eta_{\rm KT}}\ , \tag{26}$$

where $2-\eta_{\rm KT}=1.75$. The closeness of γ_p/ν_p to 1.75 is intriguing. For the Ising model, it is known that $\chi_p=\chi$ (Ref. 19) and, in $d=2$, the Ising model also has $\gamma/\nu=1.75$. However, we are not seeing a simple coincidence with the Ising behavior since $\nu_p\approx 2.5\neq\nu_{\rm Ising}=1$. But there is no theory for why $\chi_p\sim\chi$ should be true in the XY case. It would be interesting to check whether $\gamma_p/\nu_p=\gamma/\nu$ in $d>2$ where there is an ordinary critical point.

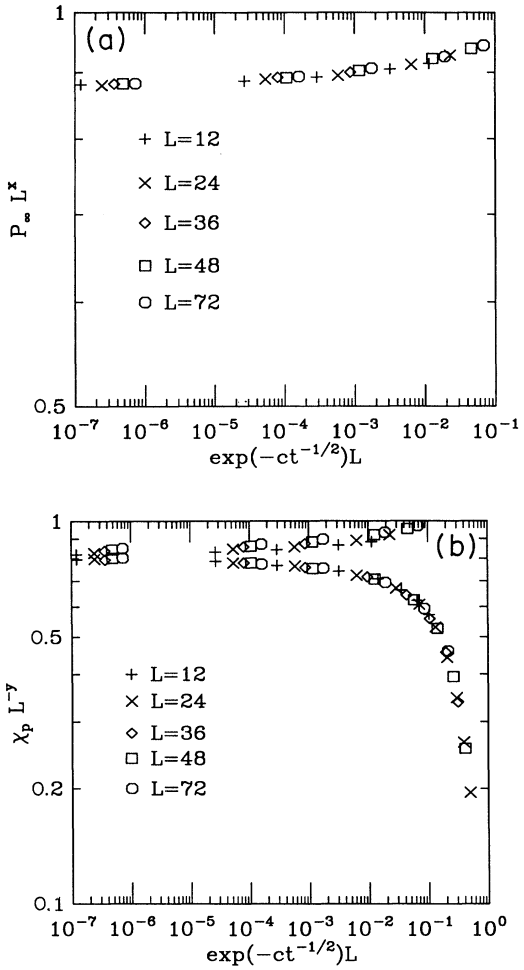

FIG. 5. Scaling plots for the FPT model using the KT form of the scaling relations.

V. CONCLUSION

By comparing our results on the AFPT and FPT models, a crucial condition for the success of the Wolff algorithm is how T_p compares with T_c. If T_p is higher than T_c, the Wolff clusters percolate before reaching T_c as the temperature is decreased, as in the case of the AFPT model, and by the time we approach the point of most interest, T_c, the algorithm is very inefficient because the clusters are mostly spanning clusters. So we want $T_p\leq T_c$. But if T_p is too low compared with T_c, the average cluster size at T_c will be small and the algorithm will not be efficient. Based on this, one would guess that the algorithm is most efficient when $T_c=T_p$, in which case spanning clusters just start to appear at T_c.

In the FPT case, the geometrical insight gained from knowledge of the percolation properties improves our understanding of exactly what kind of degrees of freedom are being updated. Furthermore, a physical picture of what is stopping the growth of the clusters would be useful for possible modifications of the algorithm to deal

with unfrustrated vector spins at $T < T_c$ (Ref. 22) or possibly with frustration.

We now consider the relation between the dynamic exponent z_W and the exponents γ_p and ν_p. Tamayo *et al.*[7] have presented essentially the same argument for the Ising case. The natural time unit for comparing computational work is one update per spin, which is proportional to the system size N. Since, in a Wolff update of a cluster of size s, only a fraction s/N of the spins are updated, and $\langle s \rangle = \chi_p$, the Wolff correlation time τ_W has to be rescaled by a factor χ_p/N [Ref. 7, Eq. (9)]. Now, let us sit at T_p and consider the time scale for updating the longest-wavelength mode. Clearly this should be related to the updates of spanning clusters. Each spanning cluster includes a fraction $\sim L^{-\beta_p/\nu_p}$ of all spins. We postulate the following assumption: when we hit each site (of order) once with a spanning cluster, the system completely forgets the old value of its longest-wavelength mode. This means we must hit a total of L^{β_p/ν_p} spanning clusters. Recall that the probability of hitting a cluster is proportional to its size; then, since the fraction of clusters we hit which are spanning is $L^{-\beta_p/\nu_p}$, we need a total of $L^{2\beta_p/\nu_p}$ Wolff hits.

However,[7] the next time a spin is hit by a spanning cluster, it is possible that this cluster comprises essentially the same sites as the previous time that the spin in question was hit; if so, this update merely undoes the effect of the earlier one. To correct for this, we must multiply the number of Wolff hits by L^{z_p}, where z_p is the dynamic exponent for the percolation correlation function which measures the overlap between how the system decomposes into clusters at times zero and t different times. This overlap is the analog of $\langle M(0)M(t) \rangle$ in a ferromagnetic spin system.

Finally, we conclude the time required to completely decorrelate the longest wavelength is

$$\tau_W = L^{2\beta_p/\nu_p + z_p} \frac{\chi_p}{N} , \tag{27}$$

i.e.,

$$z_W = [(2\beta_p + \gamma_p)/\nu_p - d] + z_p . \tag{28}$$

The result of Ref. 7 for z_W [their Eq. (15)] is the same as our Eq. (28) except it is in terms of the spin exponents, which are identical to the percolation exponents for the Ising case. Our argument shows that, more generally, the percolation exponents, not the spin exponents, must be used.

If the percolation exponents satisfy hyperscaling, as we indeed found numerically (for $d=2$) in the FPT model, then (28) gives $z_W = z_p$. More generally, if hyperscaling is violated[23] we get

$$z_W = \theta + z_p , \tag{29}$$

where $\theta \geq 0$ is the violation-of-hyperscaling exponent to be added to d in (16) and (20).

For the Ising case, the Ising spin exponents and hence the Wolff percolation exponents satisfy hyperscaling, so $z_W = z_p$. Tamayo *et al.*[7] measured the dynamic exponent $z_{\chi\chi}$ of the susceptibility correlation function $\langle \chi(0)\chi(t) \rangle$ which is apparently the percolation analog of $\langle M(0)^2 M(t)^2 \rangle$ in a spin system; this should have the same critical exponent $z_{\chi\chi} \equiv z_p$. Their numerical results show that $z_p = 0$ for the $d=4$ Ising model, but $z_p > 0$ for $d < 4$.

For vector spins, it has already been observed by Brower *et al.*[20] that $z_W = 0$ for vector spins in the upper critical dimension $d=4$. Furthermore, their numerical results[20] are consistent with $z_W = 0$ in lower dimensions. Since both terms in (29) are non-negative for physical reasons, this would imply not only that the Wolff percolation satisfies hyperscaling, but that $z_p = 0$ for all $d < 4$.

To summarize, we have found T_p and the cluster exponents for the FPT and AFPT models. In the case of the AFPT where the Wolff algorithm is unsuccessful in reducing critical slowing down, the Wolff clusters percolate at temperatures high above T_c, and the clusters are in the same universal class as random 2D percolations. In the case of the FPT where the Wolff algorithm is successful in reducing critical slowing down, we found that $T_p = T_c$ and the percolation of the Wolff clusters changed to another universal class.

ACKNOWLEDGMENTS

We would like to thank I. Clejan for sending us his Wolff algorithm code. C.L.H. is grateful to R. Brower for discussions and especially to I. Clejan and B. E. Larson for a related collaboration (Ref. 22) out of which this project developed. This research was supported by the Department of Energy Grant No. DE-FG-89ER45404.

*Present address: Supercomputer Computations Research Institute, Florida State University, Tallahassee, Florida 32306.

[1] R. Swendsen and J. S. Wang, Phys. Rev. Lett. **58**, 86 (1987).
[2] D. Kandel, E. Domany, D. Ron, A. Brandt, and E. Loh, Jr., Phys. Rev. Lett. **60**, 1591 (1988).
[3] F. Niedermayer, Phys. Rev. Lett. **61**, 2026 (1988).
[4] U. Wolff, Phys. Rev. Lett. **62**, 361 (1989).
[5] J. S. Wang, R. H. Swendsen, and R. Kotecký, Phys. Rev. Lett. **63**, 109 (1989).
[6] P. W. Kasteleyn and C. M. Fortuin, J. Phys. Soc. Jpn. Suppl. **26**, 11 (1969); C. M. Fortuin and P. W. Kasteleyn, Physica (Utrecht) **57**, 536 (1972).
[7] P. Tamayo, R. C. Brower, and W. Klein, J. Stat. Phys. **58**, 1083 (1990).
[8] E. Dagotto and J. B. Kogut, Phys. Rev. Lett. **58**, 299 (1987).
[9] G. G. Batrouni, E. R. Katz, A. S. Kronfeld, G. P. Lepage, B. Svetitsky, and K. G. Wilson, Phys. Rev. D **32**, 2736 (1985).
[10] G. G. Batrouni and E. Dagotto, Phys. Rev. B **37**, 9875 (1988); A. L. Scheinine, *ibid.* **39**, 9368 (1989); B. E. Larson and C. L. Henley (unpublished).
[11] D. Stauffer, Phys. Rep. **54**, 1 (1979).
[12] J. M. Kosterlitz and D. J. Thouless, J. Phys. C **6**, 1181 (1973); D. R. Nelson, in *Phase Transitions and Critical Phenomena,* edited by C. Domb and J. L. Lebowitz (Academic, New York,

1983), Vol. 7.
[13]D. H. Lee, J. D. Joannopoulos, J. W. Negele, and D. P. Landau, Phys. Rev. B **33**, 450 (1986). See also, S. Miyashita and H. Shiba, J. Phys. Soc. Jpn. **53**, 1145 (1984).
[14]M. P. M. den Nijs, J. Phys. A **12**, 1857 (1979).
[15]R. B. Pearson, Phys. Rev. B **22**, 2579 (1980).
[16]B. Nienhuis, E. K. Riedel, and M. Schick, J. Phys. A **13**, L189 (1980).
[17]M. Sahimi, in *The Mathematics and Physics of Disordered Media,* edited by A. Dold and B. Eckmann (Springer-Verlag, New York, 1983).
[18]F. Falo, L. M. Floria, and R. Navarro, J. Phys. Condens. Matter **1**, 5139 (1989).
[19]A. Coniglio and W. Klein, J. Phys. A **13**, 2775 (1980).
[20]R. C. Brower, N. A. Gross, and K. J. M. Moriarty (unpublished).
[21]A. Weinrib, Phys. Rev. B **29**, 387 (1984).
[22]I. Clejan, C. L. Henley, and B. E. Larson (unpublished).
[23]This occurs in the "self-organized percolation" model which has a dynamics violating detailed balance [C. L. Henley (unpublished)].